Dynamic Characteristics of a Sailplane with All-moving Tail

Justyn Sandauer, DSc, Aviation Institute, Warszawa, Poland

Presented at the 13th OSTIV Congress, Vršac, Yugoslavia (1972)

Zusammenfassung
Die Abhandlung bringt eine Diskussion des Einflusses verschiedener Parameter eines Pendelruders auf die kurzperiodischen Schwingungen eines Segelflugzeuges mit losem Knüppel. Der Einfluss der Grundparameter des Leitwerks und des Segelflugzeuges selbst auf die dynamischen Eigenschaften wurden am Beispiel des Segelflugzeuges Zefir 3 untersucht. Für diese Untersuchungszwecke wurden die folgenden Merkmale in Betracht gezogen:
- Längsstabilitätsspielraum des Segelflugzeuges
- Lage der Leitwerksdrehachse
- Massenunterausgleich des Pendel-Leitwerks
- Elastizität des Hilfsruder-Antriebssystems
- nichtlineare aerodynamische Eigenschaften des Hilfsruders im Bereich kleiner Ausschläge.

Die Berechnung wurde auf dem Solartron HS7-2 Analog-Computer durchgeführt. Der bedeutendste Einfluss auf die kurzperiodischen Schwingungsformen eines Segelflugzeuges mit losem Knüppel wird durch die Lage der Ruder-Drehachse ausgeübt. Die Grenzlage dieser Linie für die Schwingungs-Instabilität liegt vor der Grenze, bei der das Pendelruder statisch unstabil wird. Ein anderer Parameter, der einen wesentlichen Einfluss ausübt, ist die Elastizität des Hilfsruder-Systems; dieser Einfluss wächst mit der Fluggeschwindigkeit und ist ein destabilisierender Faktor. Die Untersuchungsergebnisse der Wirkung der Drehachslage des Pendelruders und seine nichtlinearen aerodynamischen Eigenschaften im Bereich kleiner Ausschläge machen es möglich, die günstigen Bedingungen für PIO (pilot induced oscillation = pilotenbeeinflusste Schwingungen) zu definieren. Wenn die Pendelruder-Drehachse hinter dem Druckpunkt liegt, ist die Aussteuerung der Schwingungen durch den Piloten schwierig wegen der umgekehrten Knüppelkraft.

Résumé
Cet article présente une discussion concernant l'influence des différents paramètres d'un empennage horizontal entièrement mobile sur les oscillations de courte durée d'un planeur «manche libre».
L'influence des paramètres fondamentaux de l'empennage et du planeur lui-même sur les caractéristiques dynamiques du planeur est analysée en prenant comme exemple le planeur Zéfir 3.
On tient compte de:
- la marge de stabilité longitudinale du planeur.
- la position de l'axe d'articulation de l'empennage horizontal.
- du balourd de l'empennage.
- de l'elasticité de la timonerie de commande du tab.
- des caractéristiques aérodynamiques non linéaires du tab pour de petits braquages.

Le calcul a été effectué sur un calculateur analogique Solartron HS7-2.
Les oscillations de courte période d'un planeur «manche libre» sont principalement liées à la position de l'axe d'articulation de l'empennage horizontal, le régime d'oscillations instables (divergentes) étant obtenu si cet axe est en avant de la position limite pour laquelle l'empennage entièrement mobile devient statiquement instable.
Un autre paramètre exerce une influence essentielle sur les caractéristiques aérodynamiques d'un planeur: c'est l'élasticité de la timonerie de commande du tab; Son effet augmente avec la vitesse de vol et est un facteur déstabilisant.
L'analyse de l'effet de la position de l'axe d'articulation de l'empennage horizontal et de ses caractéristiques aérodynamiques non linéaires pour de faibles braquages permet de déterminer les conditions favorables à un régime d'oscillations engendré par le pilote (PIO/pilot induced oscillation). Si l'axe d'articulation de l'empennage entièrement mobile est en arrière de son centre aérodynamique (foyer) les oscillations sont difficilement contrôlables par le pilote à cause de l'inversion du sens normal des efforts au manche.

1. Introduction

All-moving tails, often applied to sailplanes and aeroplanes before World War II, were neglected by the designers of light aircraft in the forties and fifties, though they were used on subsonic and supersonic aircraft. However, since 1960 the come-back of such tails has been observed in high performance sailplanes.
Simultaneously with the applications of these tails becoming more and more numerous, some theoretical papers appeared dealing with static and dynamic characteristics of a sailplane with all-moving tail.
The problem of the static characteristics was examined by Irving [1, 2], while the effect of parameters of an all-moving tail on the sailplane aerodynamic characteristics was investigated only parenthetically in Ref. [3] and [4] dealing with the phenomenon of pilot induced oscillation (PIO). This phenomenon was attributed to certain 'traps' i.e. difficulties observed in some high performance sailplanes with all-moving tails. In this connexion it seems that the problem of correct selection of parameters of an all-moving tail in order to obtain the desired flying qualities of the sailplane is not solved yet; it has to be examined, for one thing, from the point of view of the effect on the sailplane dynamic characteristics. This contribution is an excerpt from the paper prepared at the request of the Experimental Glider Establishment at Bielsko and published in Ref. [6].

2. Dynamic characteristic of the isolated all-moving tail with stick free

The first stage of the discussion on the dynamic characteristic of a sailplane with all-moving tail consists in prediction of dynamic properties of the tail itself (isolated tail). Among the all-moving tails examined by Irving [2] that with a geared tab shows the greatest margin of stability, hence the discussion on its dynamic features seems the most recommended. In addition, the conclusions obtained from that discussion can be easily adapted for tails without geared tabs, no matter if they have springs in their control systems or not.
The dynamic features of an isolated all-moving tail will be discussed first under the assumption of a rigid control system of the geared tab, then the elasticity of the control system will be taken into account. For this discussion stage the following assumptions are valid:
1. aerodynamic forces and moments are linear functions of incidence and deflection angles. The rate of change of these angles permits us to assume that the flow is quasi-steady;
2. the all-moving tail and the geared tab are mass-balanced.

Paragraph 3 deals with the effect of the two factors thus being neglected i.e. with the non-linear aerodynamic characteristic and the mass unbalance.

2.1 All-moving tail with a rigid control system of the geared tab.
Let J_T stand for the moment of inertia of the tail with respect to the hinge line. Now, the following differential equation for the undamped motion of the tail (see Fig. 1) can be written:

$$J_T \ddot{\eta} = \tfrac{1}{2}\rho V^2 S_T c_T \left[(a_1 + k a_3) x_T + k c_3\right] \Delta\eta \qquad (1)$$

The frequency of the undamped vibration is

$$\omega_n = \sqrt{-\frac{\tfrac{1}{2}\rho V^2 S_T c_T \left[(a_1 + k a_3) x_T + k c_3\right]}{J_T}} \qquad (2)$$

being in non-dimensional form

$$\bar{\omega}_n = \frac{\omega_n \ell}{V} = \sqrt{-\frac{(a_1 + k a_3) x_T + k c_3}{i_T}} \qquad (3)$$

The relation (3) shows that for increasing x_T nearing

$$x_{T\,lim} = -\frac{k c_3}{a_1 + k a_3} \qquad (3a)$$

the vibration frequency decreases, the tail becoming aperiodically unstable after having passed the limit position $x_{T\,lim}$.
Considering the very weak damping of the oscillation about the hinge line, which is close to the aerodynamic centre, one can assume that $\omega \approx \omega_n$.

2.2 All-moving tail with an elastic control system of the geared tab.
Let κ stand for stiffness coefficient of the geared tab control system. The coefficient is defined as the ratio of the moment acting upon the geared tab to the tab control system deformation measured in angle of tab deflection. Now the undamped vibration can be described by the following system of equations:

$$\left.\begin{aligned} J_T \ddot{\eta} &= \tfrac{1}{2}\rho V^2 S_T c_T \left[a_1 x_T \eta + (a_3 x_T + c_3)\beta\right] \\ J_K \ddot{\beta} &= \tfrac{1}{2}\rho V^2 S_K c_K \left[(C_{K\eta}\eta + C_{K\beta}\beta) + \varkappa(k\eta - \beta)\right] \end{aligned}\right\} \qquad (4)$$

Let us introduce the non-dimensional terms:
– moments of inertia of the tail and tab respectively

$$i_T = \frac{J_T}{\tfrac{1}{2}\rho S_T c_T \ell^2} \qquad i_K = \frac{J_K}{\tfrac{1}{2}\rho S_K c_K \ell^2}$$

– stiffness coefficient of the geared tab control system:

$$\bar{\varkappa} = \frac{\varkappa}{\tfrac{1}{2}\rho V^2 S_K c_K}$$

– time

$$\bar{t} = t\frac{V}{\ell}$$

and the operator

$$D = \frac{d}{d\bar{t}} = \frac{d}{dt}\cdot\frac{\ell}{V}$$

The following system of equations can be written:

$$\left.\begin{aligned} i_T D^2\eta - a_1 x_T \eta - (a_3 x_T + c_3)\beta &= 0 \\ (-k\bar{\varkappa} + C_{K\eta})\eta - i_K D^2\beta - (C_{K\beta} - \bar{\varkappa})\beta &= 0 \end{aligned}\right\} \qquad (5)$$

The characteristic equation of the system of equations (5) takes the form:

$$i_K i_T \lambda^4 + \left[i_T(\bar{\varkappa} - C_{K\beta}) - i_K a_1 x_T\right]\lambda^2 + a_1 x_T (C_{K\beta} - \bar{\varkappa}) - (a_3 x_T + c_3)(k\bar{\varkappa} + C_{K\eta}) = 0 \qquad (6)$$

The system is unstable if the real part of the root of the characteristic equation is positive. Now the characteristic equation can be re-written as follows:

$$\lambda^4 + C\lambda^2 + E = (\lambda^2 + \bar{\omega}_1^2)(\lambda^2 + \bar{\omega}_2^2) = 0$$

where: $\bar{\omega}_1^2 + \bar{\omega}_2^2 = C \quad \bar{\omega}_1^2 \bar{\omega}_2^2 = E$

so, the prevention of the undamped system from instability resolves itself into the condition that $\bar{\omega}_1^2$ and $\bar{\omega}_2^2$ be real and positive. If that condition is satisfied the roots of the characteristic equation become $\pm i\bar{\omega}_1$ and $\pm i\bar{\omega}_2$, and the system on being disturbed performs a motion resulting from two vibratory motions with steady amplitude and non-dimensional angular frequencies $\bar{\omega}_1$ and $\bar{\omega}_2$.
Considering the very weak aerodynamic damping of the tail motion about its hinge line one can assume that $\bar{\omega}_1$ and $\bar{\omega}_2$ are also vibration frequencies of a real system.
To get $\bar{\omega}_1^2$ and $\bar{\omega}_2^2$ real it is necessary to satisfy the condition

$$\Delta = C^2 - 4E > 0 \rightarrow E < \frac{C^2}{4}$$

while the conditions $C>0$ and $E>0$ being satisfied make $\bar{\omega}_2^1$ and $\bar{\omega}_2^2$ positive.
The coefficients C and E being substituted by the respective terms of equation (6) the following conditions are obtained for the system stability:

$$C > 0 \quad \text{whence} \quad x_T < \frac{i_T}{i_K}\cdot\frac{\bar{\varkappa} - C_{K\beta}}{a_1} \qquad (7)$$

$$E > 0 \quad \text{whence} \quad x_T < \frac{c_3(k\bar{\varkappa} + C_{K\eta})}{a_1(C_{K\beta} - \bar{\varkappa}) - a_3(k\bar{\varkappa} + C_{K\eta})} \qquad (8)$$

$$\left.\begin{aligned} &C^2 - 4E > 0 \quad \text{whence} \\ &\left[i_T(\bar{\varkappa} - C_{K\beta}) - i_K a_1 x_T\right]^2 - 4 i_T i_K \left[a_1 x_T (C_{K\beta} - \bar{\varkappa}) \right. \\ &\left. - (a_3 x_T + c_3)(k\bar{\varkappa} + C_{K\beta})\right] > 0 \end{aligned}\right\} \qquad (9)$$

The second condition ($E>0$) is equivalent to that for $x_{T\,lim}$ relating to a rigid control system of the geared tab. This equivalence can be checked by substituting $\bar{\varkappa} \rightarrow \infty$ into the right hand side of inequality (8) and by finding he limiting value after having differentiated both the numerator and denominator. As a result the following relation is obtained

$$\lim_{\bar{\varkappa}\to\infty} \frac{c_3(k\bar{\varkappa} + C_{K\eta})}{a_1(C_{K\beta} - \bar{\varkappa}) - a_3(k\bar{\varkappa} + C_{K\eta})} = -\frac{k c_3}{a_1 + k a_3}$$

For a finite stiffness of the geared tab control system the condition $E>0$ is prevailing, hence the elasticity of the geared tab control system reduces the range of hinge line positions required for stability i.e. $x_{T\,lim}$ is moved forward.
It is to be emphasized that the non-dimensional stiffness coefficient $\bar{\varkappa}$ is a function of airspeed; the increase in V is accompanied by a decrease in stiffness coefficient. In other words, for a constant stiffness the increase in airspeed causes a reduction in the range of stable x_T values.
From the two remaining conditions of the system stability the condition $C>0$ is much less severe than $E>0$, whereas the condition $E<\frac{C^2}{4}$ limits the range of stable x_T to large negative values and has no practical significance.

2.3 Example calculation. To illustrate the above statements and the effects of both the stiffness coefficient κ and airspeed on $x_{T\,lim}$ a numerical example was calculated for the all-moving tail of the Zefir-3 sailplane, the tail having the following parameters:

$S_T = 1.69\ m^2$	$a_1 = 4.42$
$S_K = 0.15\ m^2$	$a_3 = 0.67$
$c_T = 0.523\ m$	$c_3 = -0.22$
$c_K = 0.09\ m$	$C_{K\eta} = -0.2$
$k = 2.6$	$C_{K\beta} = -0.5$
$J_K = 0.03\ kgms^2 \rightarrow$	$i_T = 2.8$
$J_K = 0.0001\ kgms^2 \rightarrow$	$i_K = 0.61$

The stiffness coefficient was taken as $\kappa = 2$ m.kg/rad, being equivalent to 4 mm displacement of the tab trailing edge under the load of 1 kg. Then

$$\bar{\varkappa} = \frac{2}{\tfrac{1}{2}\rho V^2 S_K c_K} = \frac{2370}{V^2}$$

The calculations were made for 2 airspeeds:
– low airspeed V = 30 m/s
– high airspeed V = 60 m/s
and for three positions of the tail hinge line:
$x_T = -0.05;\ 0;\ 0.05$
in addition, the limit positions of the hinge line from the point of view of stability were compared for rigid and elastic control systems. The results are presented in table 1.

Table I

	rigid control system of the geared tab			elastic control system of the geared tab $\varkappa$ = 2 m.kg/rad					
V m/s				30			60		
$\bar{\varkappa}$				2,63			0,66		
$x_{T\,lim}$	0,093			0,080			0,055		
x_T	-0,05	0	0,05	-0,05	0	0,05	-0,05	0	0,05
C				5,21	5,13	5,05	1,91	1,90	1,82
E				1,39	0,855	0,32	0,375	0,195	0,015
$\Delta = C^2 - 4E$				21,6	22,8	24,2	2,42	2,94	3,26
$\bar{\omega}_1$	0,56	0,45	0,307	0,53	0,425	0,265	0,464	0,332	0,10
$\bar{\omega}_2$				2,22	2,225	2,23	1,33	1,34	1,35

3. Dynamic characteristic of the sailplane with all-moving tail with stick free

The dynamic features of the tail, described in the preceding chapter, affect directly the sailplane short period oscillations but exert no practical influence on phugoid oscillations, whose period is some tens of seconds. Hence the change of the angle of attack as well as the sailplane motion (rotation) about the lateral axis are essential parameters of the tail oscillations.

In order to explain that sort of feedback the sailplane dynamic features will be discussed below taking account of variation in geometric, mass and stiffness parameters, considering in turn the effects on the mode of short-period oscillations of a sailplane having a tail with geared tab of:

- position of the tail hinge line and the value of tab gear ratio
- elasticity of the geared tab control system
- mass unbalance
- non-linear variation of the tail hinge moment with the tail deflection angle.

Considering the margin of longitudinal stability – an essential variable parameter influencing the short-period oscillations – the discussion given below takes into account the full range of C. G. positions. The assumption of quasi-steady flow is still valid, the damping of the tail oscillations about its hinge line being neglected.

3.1 Equations of motion.

The linearized equations of the sailplane disturbed motion at constant airspeed V take the following form, where the frame of reference is fixed to the sailplane, the X-axis covers the direction of undisturbed flight, and the Z-axis is directed downwards:

$$\left.\begin{aligned}(2\mu D - C_{L_\alpha})\alpha - 2\mu\bar{q} &= 0\\ -(C_{H_{\dot\alpha}} D + C_{H_\alpha})\alpha + (i_B D - C_{H_q})\bar{q} &= 0\end{aligned}\right\} \quad (10)$$

where

$$\mu = \frac{m}{\rho S l} \qquad i_B = \frac{J_y}{\rho S l^3} \qquad \bar{q} = q\frac{l}{V}$$

$$C_{H_{\dot\alpha}} = \frac{\partial C_H}{\partial(\dot\alpha \frac{l}{V})} \qquad C_{H_q} = \frac{-\partial C_H}{\partial(q\frac{l}{V})}$$

Considering the two further degrees of freedom viz. the freedom of deflection of the tail and geared tab, we shall add to the left side of the first equation of (10) the term

$$a_1 \frac{S_T}{S}\eta + a_3 \frac{S_T}{S}\beta$$

and to the left side of the second equation the term

$$-C_{H_\eta}\eta - C_{H_\beta}\beta$$

In addition we shall introduce the equations of equilibrium of hinge moments of the tail and geared tab. Considering the mass-unbalance of the tail (that of the geared tab can be neglected) we shall introduce the additional terms into the equations of equilibrium of the tail hinge moments, consequently the linearized equation of the sailplane disturbed motion with four degrees of freedom take the following form:

$$\left.\begin{aligned}&(2\mu D - C_{L_\alpha})\alpha - 2\mu\bar{q} + a_1\tfrac{S_T}{S}\eta + a_3\tfrac{S_T}{S}\beta = 0\\ &-(C_{H_{\dot\alpha}} D + C_{H_\alpha})\alpha + (i_B D - C_{H_q})\bar{q} - C_{H_\eta}\eta - C_{H_\beta}\beta = 0\\ &-\left[(C_{H_{\dot\alpha}} - \mu_T \bar{x}_m)D + C_{H_\alpha}\right]\alpha + \left[\mu_T \bar{x}_m \bar{l}_T D - (C_{H_q} + \mu_T \bar{x}_m)\right]\bar{q}\\ &+(i_T D^2 - C_{H_\eta})\eta - C_{H_\beta}\beta = 0\\ &-(C_{K_{\dot\alpha}} D + C_{K_\alpha})\alpha - C_{K_q}\bar{q} - (C_{K_\eta} + k\bar{x})\eta + (i_T D^2 - C_{K_\beta} + \bar{x})\beta = 0\end{aligned}\right\} \quad (11)$$

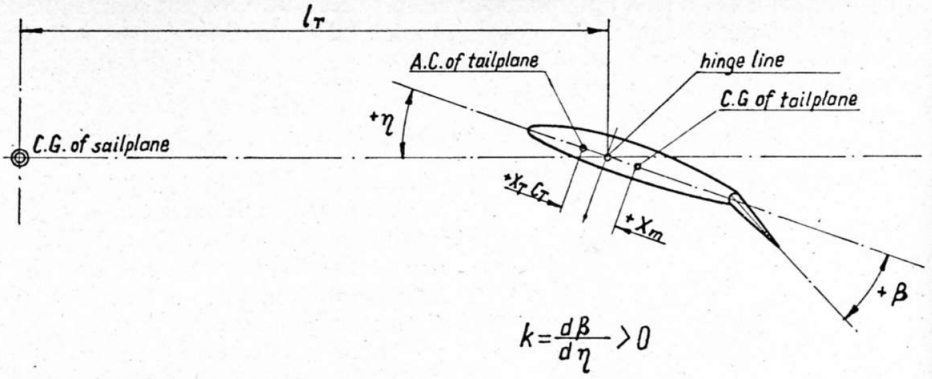

Fig. 1

where:

$$\mu_T = \frac{2m_T}{\rho S_T c_T} \qquad \bar{l}_T = \frac{l_T}{l} \qquad \bar{x}_m = \frac{x_m}{l} \text{ (see fig 1)}$$

$$C_{H_{\dot\alpha}} = \frac{\partial C_H}{\partial(\dot\alpha \frac{l}{V})} \qquad C_{H_q} = \frac{\partial C_H}{\partial(q\frac{l}{V})}$$

and analogous relations describe the derivatives of the geared tab hinge moment coefficient.

The characteristic equation of the system (11) being of sixth order, its solution requires a digital computer. A faster and clearer determination of the effect of the main sailplane and tail parameters can be obtained with aid of an analogue computer; the further investigation of the problem was performed on the Solartron HS7-2 computer.

3.2 Effect of the tail hinge line position and the sailplane margin of stability.

To make evident the coupling encountered between the sailplane oscillations and those of the tail the calculations of the disturbed motion of the Zefir-3 sailplane were carried out under the assumption of a mass balanced tail and a rigid control system of the geared tab. The investigation covered the effects of both the tail main parameter (hinge line position) and the sailplane main parameter (margin of static stability). The aerodynamic and design features of the sailplane Zefir-3 tail were described in the preceding chapter. The remaining data concerning the sailplane design and the aerodynamic derivatives included in equation (11) are as follows:

$S = 15{\cdot}7\ m^2$

$W = 510\ kg \rightarrow \mu = 60$

$J_B = 125\ kg\,m^2 \rightarrow i_B = 7{\cdot}50$

$l_T = 4{\cdot}2\ m \rightarrow \bar{l}_T = 9{\cdot}55$

$\frac{\partial \varepsilon}{\partial \alpha} = 0{\cdot}125$

$C_{L_\alpha} = 5{\cdot}69$

$C_{H_\alpha} = a_1\left(1 - \frac{\partial \varepsilon}{\partial \alpha}\right) x_T = 3{\cdot}87\, x_T$

$C_{H_{\dot\alpha}} = 2a_1 \frac{\bar{l}_T}{\bar{c}} \frac{\partial \varepsilon}{\partial \alpha} x_T = 5{\cdot}28\, x_T$

$C_{H_q} = 2a_1 \frac{\bar{l}_T}{\bar{c}} x_T = 4{\cdot}12\, x_T$

$C_{H_\eta} = a_1 x_T = 4{\cdot}42\, x_T$

$C_{H_{\dot\alpha}}$ canard $= -1{\cdot}14$

$C_{H_{\dot\alpha}}$ canard $= -0{\cdot}28$

$C_{H_{\dot\alpha}} = -2a_1 \frac{S_T \bar{l}_T^2}{S \bar{c}^2} \frac{\partial \varepsilon}{\partial \alpha} = -2{\cdot}7$

$C_{H_q} = -2a_1 \frac{S_T \bar{l}_T^2}{S \bar{c}^2} = -21{\cdot}8$

$C_{H_\eta} = -a_1 \frac{S_T \bar{l}_T}{S \bar{c}} = -2{\cdot}27$

$C_{H_\beta} = -a_3 \frac{S_T \bar{l}_T}{S \bar{c}} = -0{\cdot}34$

$C_{H_\beta} = a_3 x_T + c_3 = 0{\cdot}67\, x_T - 0{\cdot}22$

$C_{K_{\dot\alpha}} = C_{K_\eta}\left(1 - \frac{\partial \varepsilon}{\partial \alpha}\right) = -0{\cdot}175$

$C_{K_{\dot\alpha}} = 2C_{K_\eta} \frac{\bar{l}_T}{\bar{c}} \frac{\partial \varepsilon}{\partial \alpha} = -2{\cdot}38$

$C_{K_q} = 2C_{K_\eta} \frac{\bar{l}_T}{\bar{c}} = -19{\cdot}0$

The diagrams in Fig. 2 describe the sailplane response to a sudden change of angle of attack $\Delta\alpha$ or to a sudden deflection of the tail $\Delta\eta$. In the diagrams s(m) is the distance travelled in metres after the disturbance takes place. Now as a reference state for the dynamic characteristic with stick free, it is often advisable to consider that with stick fixed; it is obvious that they are the same when both the tail is fully balanced ($X_m = 0$) and the hinge line is at the tail aerodynamic centre ($X_T = 0$). Fig. 2a shows that case; a disturbance to the incidence subsides, and one to the tail results in an oscillation with neutral damping. Fig. 2b, c and d show results for other hinge line positions. For $X_T = 0.05$ the sailplane is clearly unstable, having an increasing tail oscillation, in spite of the tail in isolation being stable for X_T values up to 0.093. The limiting value of X_T that can be accepted is about 0.02 (Fig. 2b). In the diagrams the wave length of the oscillations is approximately 6.8 m and the frequency is hence about 4.5 Hη for 30 m/s and 9 Hη for 60 m/s.

The frequencies and amplitudes of the sailplane and tail oscillations depend to a very small extent upon the sailplane margin of stability. In addition, the effect of the margin of stability on the tail hinge line limit position at which the sailplane becomes unstable is imperceptible.

Additional calculations prove that the non-dimensoinal moment of inertia i_B is a parameter which exerts an essential influence on the frequency of the sailplane and tail coupled oscillations.

From the calculations carried out for the Zefir-3 sailplane, having typical design and aerodynamic features, under the above-mentioned simplifying assumptions and over the full range of hinge line positions, there were no oscillations of frequency of the order of 1 Hη, which could be associated with the PIO observed on certain types of sailplane. Those oscillations are to be detected by eliminating particular simplifying assumptions.

However, attention must be drawn to another fact shown by Fig. 2c and d, namely that the initial movements of the tail, immediately after the incidence disturbance, are in opposite directions in the two cases: with $x_T < 0$ the tail

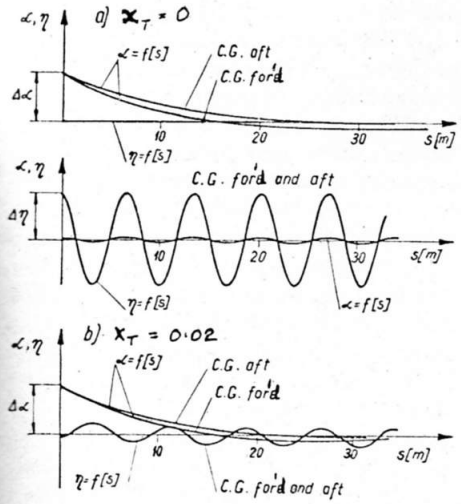

Fig. 2a

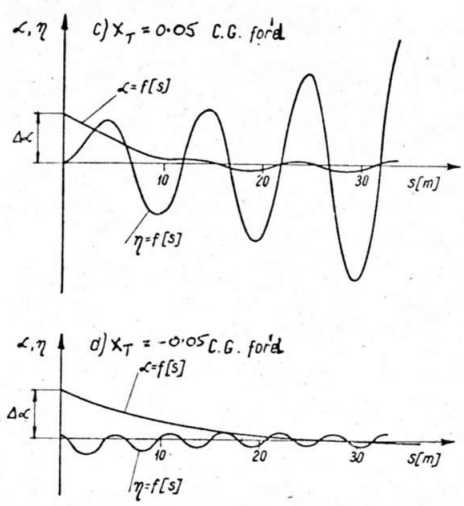

Fig. 2b

first moves trailing-edge up, as in the case of a conventional elevator, whereas with $x_T > 0$ it moves trailing-edge down, and the appearance of PIO may be connected with this fact.

Immediately after the sailplane has been disturbed through the angle $\Delta\alpha$, the direction of the tail deflection (hence the direction of the force acting on the stick) depends on the sign of x_T; for $x_T < 0$ the phenomenon is identical with that for a conventional tail, and of contrary character for $x_T > 0$.

3.3. Effect of tail mess-unbalance.

The effect of tail mass-unbalance was calculated for the Zefir-3 for two positions of the tail hinge line, the results being presented in Fig. 3. It is seen that the difference in the sailplane dynamic behaviour is insignificant even at relatively great changes of the tail C.G. position (within ± 12% of the mean aerodynamic chord). A forward displacement of the C.G. (including the position ahead of the hinge line) is a very small stabilizing factor. The frequencies are the same as in the previous case.

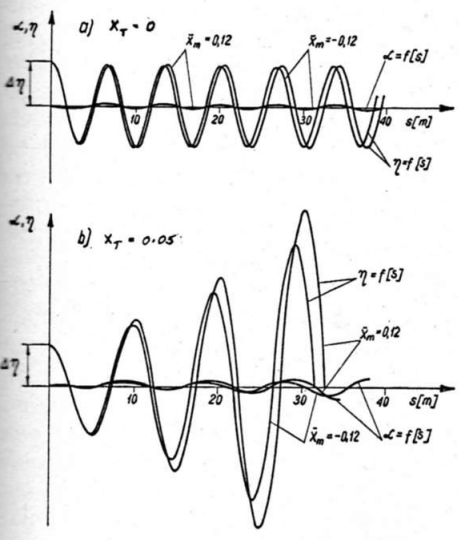

Fig 3

3.4. Effect of elasticity of the geared tab control system.

Considering the small effect of the tail C.G. position on the sailplane dynamics, as stated above, the investigation of the effect of the geared tab control system elasticity was carried out for the case of mass balanced tail. Since the effect of elasticity of the geared tab control system can depend on the tab gear ratio the calculations were made not only for the standard Zefir-3 value k = 2.6 but also k = 1.0, the lowest ratio of those examined in the course of tests on that sailplane.

To facilitate the comparison of the results with those for the isolated tail the calculations were carried out for the same airspeeds:

V = 30 m/s – low airspeed
V = 60 m/s – high airspeed

The calculation results are presented in Fig. 4 and 5. The basic conclusion drawn from the comparison of Fig. 4 with Fig. 2, b, c, d is a considerable de-stabilizing effect of elasticity of the geared tab control system. For the assumed stiffness coefficient κ = 2 m.kg/rad and for the high airspeed the consideration of elasticity of the geared tab control system results in the acceptability limit for hinge line position changing from about 0.02 to about –0.05 (although at the low airspeed the difference is only slight and 0.02 is just about acceptable. For the same elasticity of the control system a decrease in the gear ratio from k = 2.6 to k = 1.0 gives a small de-stabilizing effect and a slight increase in the oscillation period.

In the case of Fig. 5a the frequency in 1.75 Hη and in the remaining cases at varies between about 3.5 and 9.5 Hη. Therefore it can be stated that even when allowance is made for tail mass-unbalance and geared tab control system elasticity no oscillations of the order of 1 Hη frequency were observed, such as would be needed to explain the appearance of PIO.

3.5. Effect of non-linear variation of the tail hinge moment with deflection angle.

The non-linear relationship between tail hinge moment and deflection angle can concern practically two deflection ranges:

- large deflections, when the functions $C_{LT} = f(\alpha_T)$ and $C_{LT} = f(\beta)$ are non-linear
- small deflections of the tail, when the tab deflections are partially or entirely contained within the boundary layer.

Since the problem of the sailplane dynamic characteristic is discussed under the assumption of small disturbances, the interesting case of non-linear function of the tail hinge moment will be the range of small deflections. For the purposes of this paper it seems sufficient to accept a simplified model consisting of two linear functions (Fig. 6):

- for $(\eta) \leq \eta_o$ the tab deflection does not effect the tail aerodynamic coefficients
- for $(\eta) > \eta_o$ the effect of tab deflection on the tail aerodynamic characteristic is consistent with the values of derivatives a_1 and $C_{H\beta}$ accepted previously.

To explain better the effect of the tail non-linear characteristic the small gear ratio k = 1 was taken in the calculations.

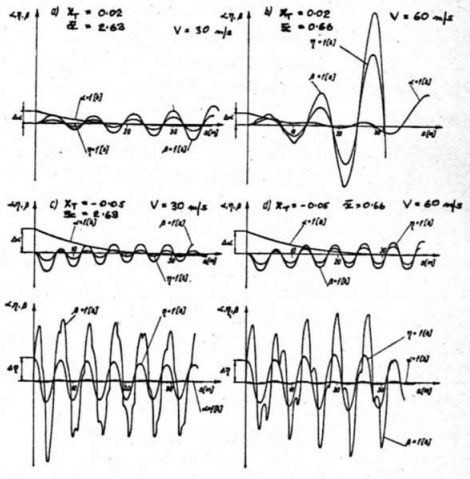

Fig. 4

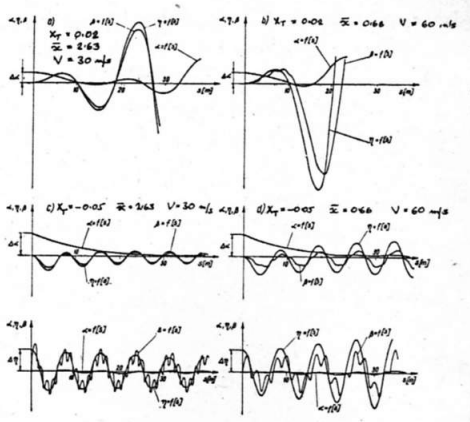

Fig. 5

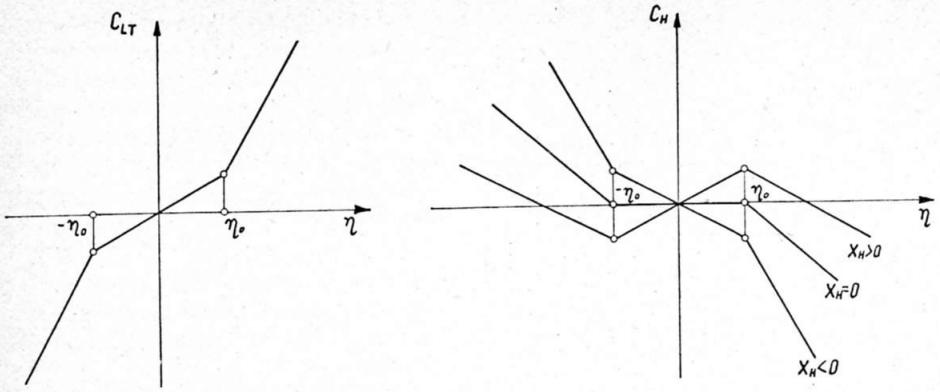

Fig. 6

The tab 'insensitivity' zone whose width is $2\eta_o$ has been related to disturbance angles $\Delta\alpha$ and $\Delta\eta$ because the characteristics of the sailplane motion depend on the ratio $\frac{\Delta\alpha}{\eta_o}$ or $\frac{\Delta\eta}{\eta_o}$.

The calculation was carried out under the assumption of a rigid control system of the geared tab. The calculation results for different positions of the tail hinge line and C.G. as well as for different values of $\frac{\Delta\alpha}{\eta_o}$ and $\frac{\Delta\eta}{\eta_o}$ are presented in Fig. 7 and 8. The changes of the above aerodynamic and design parameters involve essential changes in the disturbed motion, which is unstable for most of the cases in question. It is to be emphasized that even when the hinge line is 0.05 C_T ahead of the aerodynamic centre (Fig. 7, $X_T = -0.05$) the assumed non-linear characteristic causes instability of the sailplane motion.

Fig. 8 illustrates that ... neither the change of the sailplane margin of stability nor the change of the tail C.G. position (within the accepted C.G. displacements) exerts any essential influence on the sailplane dynamic behaviour. Special attention should be given to the case of $x_T = O$ as shown by Fig. 8. Depending on the C.G. position of the tail some poorly damped oscillations (for $\overline{x}_m < O$) or slightly divergent oscillations (for $\overline{x}_m > O$), whose frequency is a function of $\frac{\Delta\eta}{\eta_o}$, are observed. When $\frac{\Delta\eta}{\eta_o}$ decreases and nears 1 the oscillation frequency is reduced, and in the limit the oscillation decays completely. When $\frac{\Delta\eta}{\eta_o}$ increases the oscillation frequency rises and nears the value corresponding to the linear characteristic of the hinge moment (Fig. 2a), because the increasing ratio $\frac{\Delta\eta}{\eta_o}$ is equivalent to the decreasing value of η_o (at constant $\Delta\eta$). So, the non-linear case becomes nearly the linear one.

Fig. 7

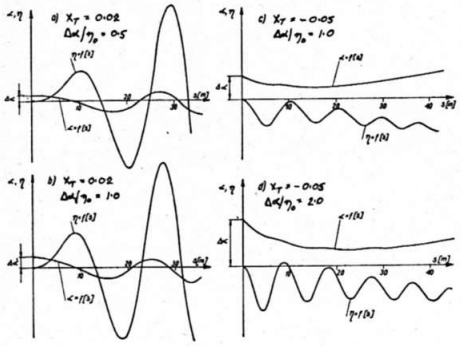

Fig. 8 also shows that for $\frac{\Delta\eta}{\eta_o} = 1.2$ and $\overline{x}_m = O$ the wave length is about 40 m corresponding, at typical operating airspeeds, to 0.5 to 1.5 Hη frequency, that is to the frequency at which PIO's are liable to occur. Although the results of the foregoing investigation on the effect of the non-linear aerodynamic characteristics of the tail on the sailplane dynamic behaviour cannot be considered sufficient for complete explanation of the occurrence of pilot induced oscillations, they do however make it possible to frame a hypothesis that pilot induced oscillations are likely when the tail hinge line is close to the tail aerodynamic centre, the condition of PIO excitation being the existing 'zone of insensitivity' of the geared tab.

It is necessary, in order to make the above hypothesis more precise and to prove it, to undertake a more detailed investigation on the effect of elasticity and clearances in the tab control system on the influence of the tail oscillation damping, and in addition it is essential to examine other models of non-linear aerodynamic characteristics of the tail.

3.6. Effect of a spring in the control system.

The effect of a spring in the control system on the sailplane dynamic behaviour depends on the spring characteristic. If the latter is linear the equations (10) remain the same, only the coefficient $C_{H\eta}$ increases viz.

$$\Delta C_{H\eta} = \frac{\alpha M_{spr}}{\alpha\eta} \frac{1}{\frac{1}{2}\varrho V^2 S_T c_T} = \frac{\text{const}}{\frac{1}{2}\varrho V^2 S_T c_T}$$

It is seen from the foregoing that $\Delta C_{H\eta}$ is a function of airspeed.

This fact is of interest in finding the solution of the equations (11). As a result we obtain the increasing wavelength of the sailplane oscillatory motion, this wavelength increase with airspeed being caused by the decrease in the coefficient $(C_{H\eta} + \Delta C_{H\eta})$.

The application of a spring having a non-linear characteristic introduces into the equations of motion the variability of $\Delta C_{H\eta}$ against η, this case being similar to that described in 3.5, while the essential influence on the motion is exerted not only by the initial disturbance but also by the airspeed.

4. **Conclusions**

The most important influence on the short-period oscillation modes of a

Fig. 8

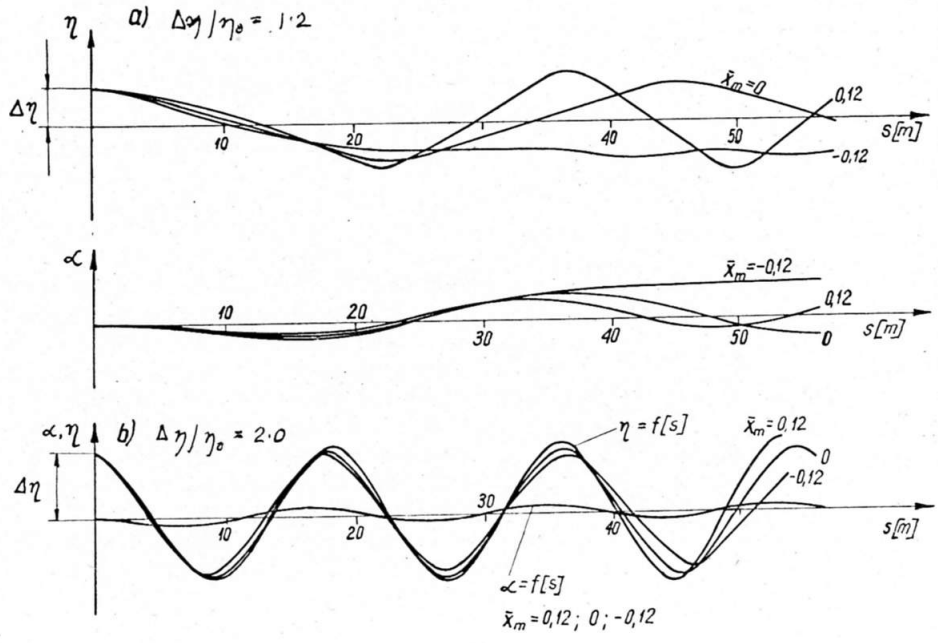

sailplane with stick free is exerted by the position of the tail hinge line, the limiting position of this line for oscillatory instability being in front of the limit at which the all-moving tail itself becomes statically unstable. Considering this fact the apparently encouraging feature of the all-moving tail with geared tab, i.e. a greater margin of stability and manoeuvrability of the sailplane with stick free at $x_T > O$, exceeding that with fixed stick, seems of doubtful practical value.

The second parameter exerting an essential effect on the sailplane dynamic characteristic is the elasticity of the geared tab control system. This effect is highly de-stabilizing and depends on the airspeed (as in case of an isolated tail). The remaining parameters under investigation have no substantial effect on the sailplane stability with stick free; however a slight stabilizing effect results from moving the tail C.G. to more forward positions, including those ahead of the hinge line.

No combination of parameters under investigation yielded any oscillations of about 1 Hη such as could be associated with pilot induced oscillations. However, it seems that the P.I.O. is connected with the relation between the direction of deflection of the tail after a disturbance of wing incidence and the tail hinge line position with respect to the tail aerodynamic centre. Immediately after a sudden change of the angle of attack the direction of deflection of the tail (and, consequently, the direction of force acting upon the control stick) depends on the sign of x_T. For $x_T < O$, the phenomenon is identical with that for a conventional tail, the opposite effect occurring for $x_T > O$. Allowance for non-linear tail hinge moment characteristics shows a de-stabilizing effect. The frequency of the oscillations, which are slightly damped or slightly divergente according to whether the tail C.G. is ahead of or oft of the hinge line, is a function of the ratio $\Delta\eta/\eta_o$, and can be in the range characteristic of P.I.O.

Summarising, the results of this work make it possible to frame the hypothesis that pilot induced oscillations may appear when the tail hinge line is close to the tail aerodynamic centre, the condition of excitation being the existing 'zone of insensitivity' of the geared tab. When the tail hinge line is a little behind the aerodynamic centre the damping of oscillations by the pilot is difficult because of the reverse stick force.

To prove this hypothesis and to be more precise, the effects of elasticity and clearances in the tab control system need to be determined in more detail, and other models of the non-linear tail characteristics should be investigated.

References

1. Irving F. G.: All moving tailplanes. OSTIV Publication VII, 1963
2. Irving F. G.: The stick – force/speed characteristics of various types of tails and elevator trimmers. OSTIV Publication X, 1968
3. Irving F. G.: PIO's in gliders. Sailplane and Gliding, February–March, 1969
4. Gibson J. C.: Some notes on handling qualities. Sailplane and Gliding, August–September, 1969
5. Etkin B.: Dynamics of flight. John Wiley and Sons. New York 1959
6. Sandauer J.: Static and dynamic characteristics of a sailplane with all-moving tail. Prace Instytutu Lotnictwa no. 47, 1971

More important notation

a_1	derivative of the tail lift coefficient with respect to the angle of attack
a_3	derivative of the tail lift coefficient with respect to the geared tab deflection angle
$C_{L\alpha}$	derivative of the lift coefficient with respect to the angle of attack
$C_{m\alpha}$	derivative of the pitching moment coefficient with respect to the angle of attack
$C_{m\alpha}'$	derivative of the pitching moment coefficient with respect to the non-dimensional rate of change of the angle of attack
C_{mq}	derivative of the pitching moment coefficient with respect to the non-dimensional rate of rotation about the lateral axis
$C_{m\eta}$, $C_{m\beta}$	derivatives of the pitching moment coefficient with respect to the angles of deflection of the tail and geared tab respectively
C_{LT}	tail lift coefficient
C_H, C_K	tail and geared tab hinge moment coefficients
$C_{H\alpha}$, $C_{K\alpha}$	derivatives of tail and geared tab hinge moment coefficients with respect to the angle of attack
$C_{H\alpha}'$, $C_{K\alpha}'$	derivatives of tail and geared tab hinge moment coefficients with respect to the non-dimensional rate of change of the angle of attack
$C_{H\eta}$, $C_{H\beta}$	derivatives of the tail hinge moment coefficient with respect to the angles of deflection of the tail and geared tab respectively
C_{Hq}, C_{Kq}	derivatives of tail and geared tab hinge moment coefficients with respect to the non-dimensional angular velocity in pitch
$C_{K\eta}$, $C_{K\beta}$	derivatives of tail and geared tab hinge moment with respect to the tail and tab deflection angles
c_T, c_K [m]	mean aerodynamic chords of the tail and geared tab
c_3	derivative of the tail pitching moment with respect to the geared tab deflection angle
J_y [m.kg.sec^2]	moment of inertia of the sailplane about the lateral axis
J_T, J_K [m.kg.sec^2]	tail and geared tab moment of inertia about the hinge line
i_B, i_T, i_K	moments of inertia I_y, I_T, I_K in non-dimensional form
k	tab gear ratio
l [m]	reference length
l_T [m]	tail arm
$\bar{l}_T$	tail arm in non-dimensional form
m [kg.sec^2/m]	sailplane mass
m_T [kg.sec^2/m]	tail mass
q [rad/sec]	angular velocity in pitch
$\bar{q}$	angular velocity q in non-dimensional form
S [sq.m]	wing area
S_T, S_K [sq.m]	tail area, tab area
t [sec]	time
$\bar{t}$	time in non-dimensional form
V [m/sec]	airspeed
W [kg]	sailplane weight
w [m/sec]	airspeed component along the sailplane vertical axis
x_T	distance of the tail hinge line from the tail aerodynamic centre as measured in mean aerodynamic chords c_T
x_m [m]	distance of the tail hinge line from the tail centre of gravity
$\bar{x}_m$	distance x_m in non-dimensional form
α [rad]	sailplane angle of attack
α_T [rad]	tail angle of attack
η, β [rad]	tail and geared tab deflection angles
ε [rad]	downwash angle at tail
κ [m.kg/rad]	stiffness coefficient of the geared tab control system
$\bar{\kappa}$	coefficient κ in non-dimensional form
μ	sailplane relative mass
ϱ [kg.sec^2/m^4]	air density
ω [rad/sec]	angular frequency
$\bar{\omega}$	angular frequency ω in non-dimensional form.